

1 **A simple, sensitive and quantitative FACS-based test**  
2 **for SARS-CoV-2 serology in humans and animals**  
3

4 Agnès Maurel Ribes<sup>1+</sup>, Pierre Bessière<sup>2+</sup>, Jean Charles Guéry<sup>3</sup>, Eloïse Joly  
5 Featherstone<sup>4</sup>, Timothée Bruel<sup>5</sup>, Remy Robinot<sup>5</sup>, Olivier Schwartz<sup>5</sup>, Florence  
6 Abravanel<sup>3,6</sup>, Jacques Izopet<sup>3,6</sup> and Etienne Joly<sup>7\*</sup>  
7

8 1 : Laboratoire d’Hématologie, Centre Hospitalier Universitaire de Toulouse,  
9 31000, Toulouse, France

10 2 : Ecole nationale vétérinaire de Toulouse, Université de Toulouse, ENVT, INRAE,  
11 IHAP, UMR 1225, Toulouse, France

12 3 : Institut Toulousain des Maladies Infectieuses et Inflammatoires (Infinity),  
13 Université de Toulouse, INSERM, CNRS, UPS, 31300 Toulouse, France

14 4 : York University Hospital, York YO31 8HE, UK

15 5: Institut Pasteur, Virus and Immunity Unit, CNRS-UMR3569, Paris, France

16 6: Université de Toulouse, INSERM, CNRS, UPS, 31300 Toulouse, France

17 7: Institute of Pharmacology and Structural Biology (IPBS), University of Toulouse,  
18 CNRS, Toulouse, 31000, France  
19

20 +: AMR and PB made equivalent contributions to this work.

21 \*: correspondence to EJ: [atnjoly@mac.com](mailto:atnjoly@mac.com)  
22

## 23 **Abstract**

24 Serological tests are important for understanding the physiopathology and following the  
25 evolution of the Covid-19 pandemic. Assays based on flow cytometry (FACS) of tissue culture  
26 cells expressing the spike (S) protein of SARS-CoV-2 have repeatedly proven to perform slightly  
27 better than the plate-based assays ELISA and CLIA (chemiluminescent immuno-assay), and  
28 markedly better than lateral flow immuno-assays (LFIA).

29 Here, we describe an optimized and very simple FACS assay based on staining a mix of two  
30 Jurkat cell lines, expressing either high levels of the S protein (Jurkat-S) or the mCherry  
31 fluorescent protein (Jurkat-R, which serve as an internal negative control). We show that this  
32 Jurkat-S&R-flow test has a much broader dynamic range than a commercial ELISA test and  
33 performs at least as well in terms of sensitivity and specificity. Also, it is more sensitive and  
34 quantitative than the hemagglutination-based test HAT, which we described recently. The  
35 Jurkat-R&S-flow test requires only a few microliters of blood; thus, it can be used to quantify  
36 various Ig isotypes in capillary blood collected from a finger prick. It can be used also to evaluate  
37 serological responses in mice, cats and dogs. FACS tests offer a very attractive solution for  
38 laboratories with access to tissue culture and flow cytometry who want to monitor serological  
39 responses in humans or in animals, and how these relate to susceptibility to infection, or re-  
40 infection, by the virus, and to protection against Covid-19.

41

## 42 **Introduction**

43 Over the past year, our world has been thrown into disarray by a pandemic caused by a new  
44 coronavirus, SARS-CoV-2. With a mortality rate around 1%, this new virus is not as pathogenic as  
45 previous coronaviruses such as SARS-CoV (9.6%) and MERS (35%), but it transmits faster from  
46 human-to-human (Fani et al. 2020), probably because of a large proportion (ca. 50%) of  
47 asymptomatic carriers (Wu et al. 2021; Long et al. 2020). Consequently, in less than two years  
48 since its discovery in Wuhan, China, SARS-CoV-2 has spread all over the world and caused more  
49 than 200 millions confirmed cases and over 4 millions confirmed deaths (  
50 <https://www.who.int/emergencies/diseases/novel-coronavirus-2019> ).

51 Biotechnology has proven a great asset in combating the pandemic, with the rapid  
52 development of diagnostic tests and, more recently, of vaccines. Diagnostic tests detect directly  
53 either the viral nucleic acid or viral proteins in nasopharyngeal swabs. Serological tests, by  
54 contrast, detect antibodies developed in response to infection by the virus or vaccination, or a  
55 combination of the two. Since the presence of antibodies in serum usually correlates with  
56 elimination of the virus and the patient's recovery, serological tests have not been very helpful  
57 in the clinic. They have, however, proven an essential tool to follow the spread of the pandemic  
58 by evaluating seroprevalence in populations, and they are now set to become essential to  
59 evaluate the immunity of individuals as well as populations (Koopmans and Haagmans 2020).

60

61 Whilst several thousands of studies have been published by now, based on serological tests  
62 performed in many millions of individuals, those myriad studies mostly document the  
63 seroprevalence in certain populations at a given time (Chen et al. 2021), but information  
64 regarding the actual protection afforded by immunity after infection by SARS-CoV-2, and how  
65 this correlates with the presence of antibodies against the SARS-2 virus is only just starting to  
66 come out (Lumley et al. 2021; Letizia et al. 2021; Abu-Raddad et al. 2021; Jeffery-Smith et al.  
67 2021; R. A. Harvey et al. 2021; Garcia-Beltran et al. 2021). ).

68 While these recent publications show that the presence of antibodies does correlate with  
69 protection against the Covid-19 disease, and in particular against the more serious forms of the  
70 disease, one of the more burning questions that remains to be answered is how long this  
71 protection will last? Another crucial question concerns whether there will be differences in the  
72 duration of this protection depending on which vaccine was used, and whether an individual  
73 had been infected by the SARS-CoV-2 virus before being vaccinated.

74  
75 Obtaining answers to this type of questions should be greatly facilitated by access to simple,  
76 cheap and quantitative serological tests, which would work both in humans and in animal  
77 models. To date, however, although a multitude of commercial serological tests have been  
78 developed to detect the presence of antibodies in the serum of patients (Farnsworth and  
79 Anderson 2020), those are mostly ill-suited for use in research laboratories, not only because of  
80 their price, but also because they are not or only poorly quantitative.

81  
82 The most commonly used methods for Covid-19 serodiagnostic are either ELISA (Enzyme-  
83 Linked ImmunoSorbent Assays) or CLIA (ChemiLuminescent ImmunoAssays). Whilst those  
84 methods show very good sensitivity and specificity, they also have several significant  
85 drawbacks:

- 86 i) The commercial versions are based on using volumes of serum or plasma which exceed the  
87 amounts which can be readily obtained by finger prick, and therefore require venipuncture,  
88 and hence trained personnel to collect the samples, and elaborate logistics to handle those  
89 samples.  
90 ii) They are relatively expensive (ca. 500 € per plate of 90 tests for commercial ELISA or CLIA )  
91 and not easily modular (i.e. a whole plate will often have to be used even if only a few tests  
92 are to be performed). Whilst in-house ELISAs are a possible alternative, they are difficult to  
93 standardize and require high amounts of recombinant antigen (Amanat et al. 2020).  
94 iii) Whilst ELISA tests are quantitative, they tend to saturate rapidly, and thus show a relatively  
95 limited dynamic range.  
96 iv) Most commercial versions are designed to detect human antibodies, and thus cannot be  
97 used to follow serological responses in animal models.

98  
99 Early in the pandemic, because they could be used in a point of care setting on capillary  
100 blood obtained by finger pricks, lateral-flow immune assays (LFIA) attracted considerable  
101 attention as an alternative to the ELISA or CLIA plate-based methods. Dozens of versions were  
102 developed by various commercial companies, and despite their relatively high price, such LFIAs  
103 were used in scores of studies to evaluate the prevalence of sero-conversion in various  
104 populations. Over time, however, the general performances of LFIAs have proven to be too low,  
105 both for sensitivity and reliability, to be of real use in clinical settings, and even for  
106 epidemiological studies (Adams et al. 2020; Mohit et al. 2021; Dortet et al. 2021; Moshe et al.  
107 2021).

108  
109 As an alternative to those various serological tests, we set out to develop a serological test  
110 based on hemagglutination, with the aim of obtaining a method that would be both sensitive,  
111 cheap, and could be used both in the laboratory, in field settings or as a point of care test,  
112 without the requirement for any elaborate equipment. The HAT (HemAgglutination Test)  
113 method is based on a single reagent, IH4-RBD, which binds to human red blood cells (RBC) via

114 the IH4 nanobody specific for human Glycophorin A and coats them with the RBD domain of the  
115 SARS-CoV-2 virus (Townsend et al. 2021). HAT has a sensitivity of 90% and specificity of 99%,  
116 and is now used by several laboratories worldwide for epidemiological and clinical studies  
117 (Kamaladasa et al. 2021; Jayathilaka et al. 2021; Jeewandara et al. 2021). To be able to perform  
118 HAT on whole blood with the sensitivity and simplicity which we set out the reach, and to  
119 attempt to make it quantitative, various modifications and improvements had to be tested, and  
120 in order to do this, we felt that we needed a simple quantitative test that would allow us to  
121 evaluate the amount of antibodies present in the whole-blood samples we were using more  
122 simply and cheaply than by using ELISA or CLIA.

123

124 In this regard, the S-flow test (Grzelak et al. 2020), which uses flow cytometry (FACS)  
125 performed on human cells expressing the S protein, appeared as a very promising approach  
126 since it is very simple to run and its performances compared favorably with three other  
127 serological tests (two ELISA directed towards the S or N proteins, and a luciferase immuno-  
128 precipitation system (LIPS) combining both N and S detection).

129 The S-flow method initially described used HEK cells (Grzelak et al. 2020), which are adherent  
130 cells. We felt that it would be better to use cells growing in suspension, not only because it  
131 makes it a lot easier to grow large numbers of cells, but also because those can be used directly,  
132 without having to be detached from the plastic, which we feared could possibly alter the cells'  
133 characteristics, and introduce a possible source of variability between assays.

134 In this regard, Horndler and colleagues have recently described an assay inspired by the S-  
135 flow assay, but based on Jurkat cells expressing both the full-length native S-protein of SARS-  
136 CoV-2 and a truncated form of the human EGFR protein, which is used as an internal control for  
137 the expression level of the S protein (Horndler et al. 2021).

138 One of the caveats of using human cells to express the S protein, however, is that those cells  
139 will also express other antigens, and MHC molecules in particular, which can be the targets of  
140 allo-reactive antibodies present in certain individuals, and not others. The background level of  
141 staining on Jurkat cells themselves will thus vary from sample to sample. To circumvent this  
142 difficulty, Pintero et al. have used the Jurkat-S+EGFR cells mixed with untransfected Jurkat cells  
143 as negative controls (Piñero et al. 2021).

144 Having followed the same reasoning as Horndler *et al.*, we had chosen to make use of Jurkat  
145 cells expressing the native form of the spike protein of the SARS-CoV-2 virus, but we elected to  
146 use Jurkat cells expressing the mCherry red fluorescent protein as negative controls. This is not  
147 only cheaper because it does not require labelling the cells with an additional commercial  
148 antibody, but also has the advantage of using two cell lines that are maintained in the same  
149 selective tissue culture medium.

150 In all three papers (Horndler et al. 2021; Piñero et al. 2021; Grzelak et al. 2020), and several  
151 others (Egia-Mendikute et al. 2021; Hambach et al. 2021; Lapuente et al. 2021; Goh et al. 2021),  
152 the sensitivity of approaches based on flow cytometry was reported to be superior to those of  
153 ELISA or CLIA, probably because such tests are based on detecting the spike protein expressed  
154 in its native conformation.

155 Since the Jurkat-R&S-flow test calls for the use of both a flow cytometer and cells obtained  
156 by tissue culture, it is clearly not destined to be used broadly in a diagnostic context, but its  
157 simplicity, modularity, and performances both in terms of sensitivity and quantification  
158 capacities should prove very useful for research labs working on characterizing antibody  
159 responses directed against SARS-2, both in humans and animal models.

## 160 **Results and Discussion**

161

### 162 ***Jurkat-S&R-flow: basic principles***

163

164 Jurkat cells expressing high levels of the SARS-CoV-2 spike protein, which we subsequently  
165 refer to as Jurkat-S, or J-S, were obtained by means of transduction with a lentiviral vector,  
166 followed by three rounds of cell sorting. A second population of Jurkat cells, in which all cells  
167 express the mCherry fluorescent protein, and which we subsequently refer to as Jurkat-R, or J-R,  
168 was also obtained by lentiviral transduction (see M&M: Materials and Methods section).

169

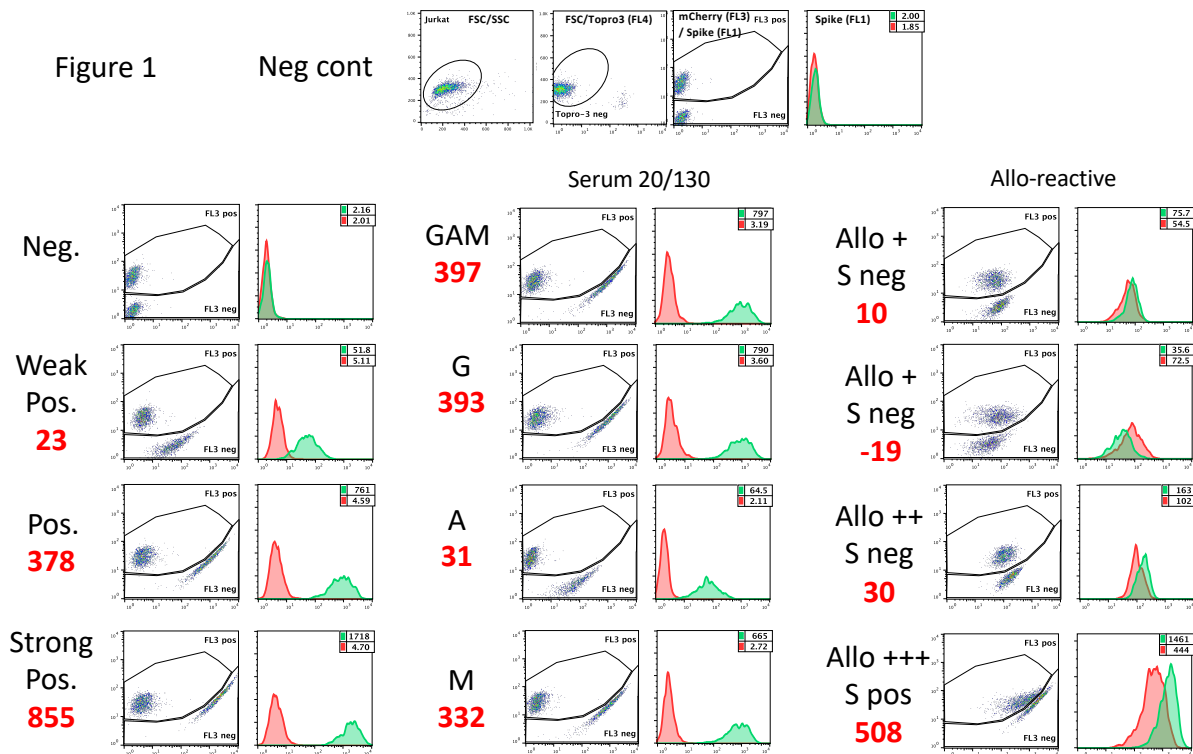
170 For the Jurkat-S&R-flow test, we simply prepare a mix of equivalent numbers of the two cells  
171 lines, J-S and J-R, and use either sera or plasma at a final dilution of 1/100 to label  $2 \cdot 10^5$  cells of  
172 this mix (see M&M for details). After this primary step of labelling, the cells are washed before  
173 being incubated with a fluorescent secondary antibody, and a final wash is performed before  
174 analysis by flow cytometry.

175

176 The advantage of using such an approach is that it guarantees that the test cells (Jurkat-S)  
177 and the control cells (Jurkat-R) are labelled in exactly the same conditions. Comparing the levels  
178 of staining between test and control cells can then be carried out without any risk of a  
179 difference between the two being due to a difference in the course of the labelling procedure  
180 (e.g. less of the primary or secondary antibodies). Accessorily, another significant advantage of  
181 such an approach is that it reduces the number of FACS samples to be processed by a factor of  
182 two.

183

184 The mCherry signal allows simple separation by gating during analysis of the control cells  
185 from the test cells (Figure 1). In samples labelled just with the secondary antibody (neg. cont.)  
186 or with pre-pandemic plasma which does not contain antibodies against the spike protein (neg  
187 plasma), similar green signals are found on J-S et J-R populations. When there are antibodies  
188 against the spike protein present in the plasma or serum used to label the cells, this will result in  
189 a marked difference in the green signals detected on the J-S cells compared to the J-R cells. The  
190 difference in the fluorescence intensity between the two populations will provide a quantitative  
191 evaluation of the amounts of antibodies in the serum or plasma used to label the cells (first  
192 column). The numbers shown in red correspond to the relative specific staining (RSS = signal J-S  
193 – signal J-R / signal neg. cont.).



194  
195

196

197

198

199

200

201

202

203

204

205

206

207

208

209

210

211

212

213

214

215

216

217

218

219

220

221

222

**Figure 1: Basic principle and examples of the Jurkat-S&R-flow test**

A 50/50 mix of Jurkat cells expressing either the S protein of the SARS-CoV-2 virus or the mCherry protein is first incubated with a 1/100 dilution of the plasma or serum sample to be tested, followed by incubation with a green fluorescent secondary antibody. The cells are then analyzed by flow cytometry.

The panels on the first line show the gating strategy, using as an example the sample of a negative control, stained only with an anti-human pan specific secondary antibody conjugated to alexa-488 : Live cells are first selected on a combination of two gates drawn on three parameters: size (FSC), granularity (SSC), and far red fluorescence (FL4) to eliminate the dead cells labelled by the Topro3 live stain. Jurkat-S are then distinguished from Jurkat-R cells using the red fluorescence of the latter, by means of a gate drawn on a FL1/FL3 dotplot. The gates had to be drawn that way to accommodate the fact that, for the brightest cells, the green fluorescent signal of alexa-488 can 'bleed' into the FL3 channel, and the Cellquest software does not allow for FL3/FL1 compensation. A histogram overlay is then drawn with the cells falling in each of these two gates (red: Jurkat-R, green: Jurkat-S). The numbers in the upper right corners of those histograms correspond to the GMFIs of the two histograms.

The red numbers shown to the left of the plots correspond to the relative specific staining (RSS; i.e. the difference of signal between J-S and J-R divided by the GMFI of the negative control, i.e. 2.00)

The first column shows examples of staining with 4 different plasmas which were either negative, or weakly, positively and strongly reactive with the spike protein.

The second column shows an example of the Jurkat-S&R-flow test capacity to perform a rough evaluation of the relative proportion of the various Ig isotypes in a sample, in this case the 20/130 reference serum obtained from the NIBSC.

The third column presents examples of some of the rare samples which showed various levels of allo-reactivity against the Jurkat cells themselves. Although the sample on the third line had an RSS of 30 (thus well above the threshold of 20 set for positivity), this sample was probably negative since it showed no reactivity in the other two serological tests. The sample on the fourth line shows that some sera can be both allo-reactive against the Jurkat cells, and strongly reactive against the spike protein.



223 If isotype-specific secondary reagents are used, an evaluation of the respective amounts of  
224 various classes of antibodies can also be obtained (second column). It should, however, be  
225 noted that, because different secondary reagents do not necessarily recognize the various Ig  
226 isoforms with the same efficiency, this provides only a very rough analysis of the relative  
227 amounts of Ig-G, -A and -M. Within a set of samples, however, this can provide very simple  
228 means to compare samples with one another (Table S1).

229  
230 As alluded to in the introduction, one of the possible caveats of using a human cell line to  
231 express the S protein is that some blood samples will contain allo-reactive antibodies directed  
232 against that cell line, possibly as a consequence of a pregnancy, or past history of receiving a  
233 blood transfusion or organ transplant (Hickey et al. 2016; Karahan et al. 2020). The third column  
234 of Figure 1 shows examples of such samples containing marked levels of alloreactive antibodies,  
235 i.e. samples for which the J-R cells show significant levels of staining compared to the same cells  
236 labelled with just the secondary antibody. Based on our results collected on more than 350  
237 clinical samples, we evaluate that ca. 30 % of samples will contain allo-reactive Abs that will  
238 result in levels of staining of Jurkat cells that are more than five-fold that of the signal obtained  
239 for the negative control (and 3-6 % more than ten-fold). Of note, we did not notice an increased  
240 frequency of allo-reactivity in samples from women compared to men, which suggests that allo-  
241 reactivity after pregnancy is not a major cause in the origin of those allo-reactions.

242  
243 A difficult question with all serological tests is that of where to set the threshold beyond  
244 which the specific signals detected can confidently be considered as positive, which will be  
245 directly linked to the balance between sensitivity and specificity of the assay. Based on the  
246 analyses of various cohorts of positive and negative samples (some of which will be presented  
247 further down in this manuscript), for the Jurkat-S&R-flow, we have settled for a threshold of RSS  
248 =20, i.e. twenty-fold the value of the negative control stained just with secondary-antibodies.  
249 The reason for using the geometric mean of fluorescence intensity (GMFI) of the negative  
250 control as an internal reference is that, in flow cytometry, the numerical values of fluorescence  
251 intensities will be totally dependent upon the cytometer settings, and the voltages applied to  
252 the PMT in particular. But we find that this can be somewhat compensated by such an  
253 approach. For example, in the conditions used in our experiments, the geometric mean of  
254 fluorescence intensity (GMFI) of the negative control had a value of ca. 2 when analyzed on a  
255 FACScalibur flow cytometer. With a threshold set at 20, samples were thus considered as  
256 positive if the difference in the GMFI of the J-S and J-R populations was above 40 (numbers  
257 shown in red in Figure 1 are  $J-S - J-R / 2$ ). When the very same samples were analyzed on a  
258 Fortessa flow cytometer (Figure S1), the value of the GMFI for the negative control was 24-fold  
259 higher, but the RSS values obtained closely resembled those obtained with the same samples on  
260 the FACScalibur (red numbers in Figure S1 and Figure 1: 20/23; 366/378; 916/855; 490/508).

261  
262 For the samples showing high levels of allo-reactive staining, however, it is worth underlining  
263 that this threshold of 20 had to be considered with some caution. Indeed, in those allo-reactive  
264 samples, such as the examples shown in the right column of Figure 1, we found that the  
265 difference between the green signals recorded for the J-S and J-R populations can fluctuate  
266 between experiments, presumably because those signals correspond to the recognition by allo-  
267 reactive antibodies of cell surface markers that are not always expressed at the same levels in  
268 all Jurkat cells. Such alloreactive signals can be higher in J-R for certain serum or plasma

269 samples, or in J-S for other samples (first vs second and third line), without, in this latter case,  
270 necessarily corresponding to bona-fide reactivity against the spike protein of the SARS-CoV2  
271 virus. The sample shown on the fourth line represents the most extreme case we have come  
272 across, from a Covid-19 patient with extremely high allo-reactivity, coupled to bona fide  
273 reactivity against the spike protein. All in all, it is simply worth underlining that, for the small  
274 percentage of samples showing significant alloreactivity against Jurkat cells, and staining of  
275 Jurkat-S slightly higher than that of Jurkat-R, their reactivity should be checked with a different  
276 serological test before considering them as truly positive.

277  
278 Inspection of the dot plot for this very alloreactive sample provides the explanation for the  
279 slightly odd shapes of the FL1/FL3 gates we used to discriminate Jurkat-S from Jurkat-R cells.  
280 This was necessary because, on the FACScalibur, the fluorescent signal of mCherry is best  
281 captured by the FL3 channel, but the version of the Cellquest program used for acquisition on  
282 this cytometer does not allow for FL3/FL1 compensation. Consequently, samples with extremely  
283 high FL1 signals showed some 'bleeding' into the FL3 channel. We found that this could not be  
284 satisfactorily treated by post-acquisition compensation with the Flowjo analysis software either,  
285 and thus resorted to drawing such gates to separate J-S from J-R populations.

286  
287 We had elected to use a green/red combination for test and control cells for two reasons: 1)  
288 secondary antibodies labeled with green fluorescent dyes such as fluorescein or Alexa 488 are  
289 the most commonly available, and also usually the cheapest. 2) All flow-cytometers, even the  
290 most basic ones, are equipped with a 488 nm laser which allows to perform green/red analyses.  
291 Another important consideration is that one of the goals of this study was to set up a test which  
292 could be used by as many research teams as possible, including those based in institutes from  
293 less affluent countries, which are less likely to have access to recent, state-of-the-art multi-laser  
294 flow cytometers.

295  
296 When the same samples as shown on Figure 1 were analyzed using a Fortessa flow  
297 cytometer, the picture was quite different (Figure S1). This more recent flow cytometer is  
298 endowed with several lasers, including a 561 nm Yellow-Green laser, which is much better  
299 suited for the excitation of the mCherry fluorescent protein, thus yielding much higher signals  
300 which, since they are acquired on a different laser line from the green signals, require absolutely  
301 no compensation.

302  
303 In many flow cytometry facilities, users are required to fix any samples that have been in  
304 contact with materials of human origin. Whilst this was not the case for us, we still tried  
305 analyzing the same samples after those were fixed with 1% formaldehyde and kept for 4 days at  
306 4°C before re-analysis. As can be seen on the right part of Figure S1, formaldehyde-fixation  
307 resulted in a 7-fold drop in the intensity of the mCherry signals, which made it impossible to  
308 separate J-R from J-S population on the FACScalibur (first line). On the other hand, analysis on  
309 the Fortessa was still comfortably possible. Of note, whilst formaldehyde did not noticeably  
310 alter the fluorescence signals of the alexa-488 dye, it did result in a twofold increase of the  
311 green auto-fluorescence of the negative controls, hence resulting in a twofold reduction of the  
312 RSS compared to those obtained on unfixed cells.

313  
314



315 **Performance of the JurkatS&R-flow test on clinical samples**

316  
317 Next, we compared the performance of the Jurkat-S&R-flow test with those of two other  
318 serological tests: the Wantai commercial RBD ELISA test, and the hemagglutination-based test,  
319 HAT (Townsend et al. 2021).

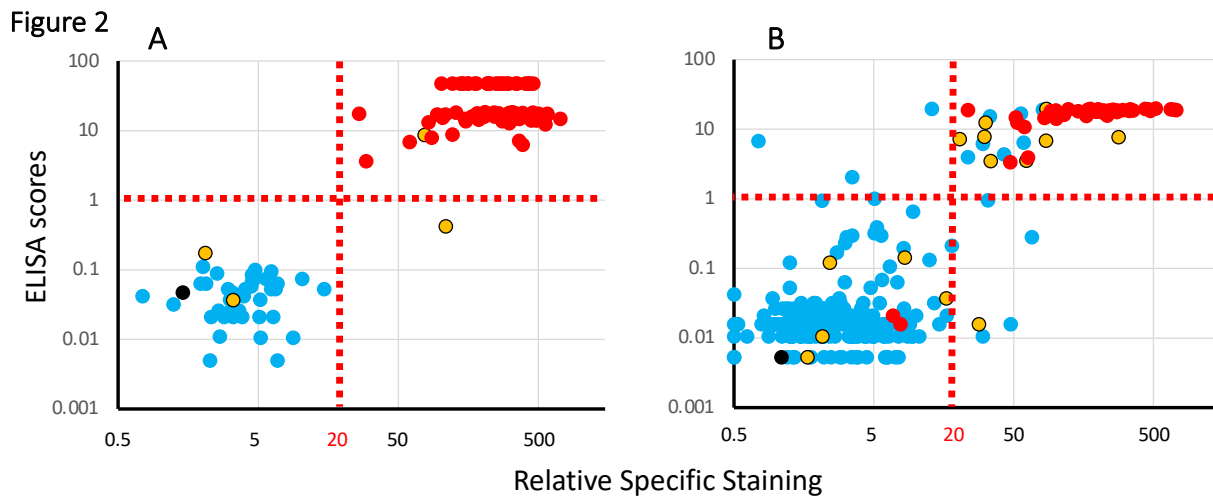
320  
321 For this, we made use of two cohorts of clinical samples.

322 First, a preexisting cohort of 121 sera available in the virology laboratory of the Toulouse  
323 hospital which had all previously been tested with the Wantai RBD ELISA test (Abravanel et al.  
324 2020), comprising 40 negative serum samples collected before December 2020, and 81 sera  
325 from PCR-positive subjects. For those samples, RBCs from O- donors were used to perform the  
326 HAT tests (see M&M).

327 The second cohort consisted of 267 whole blood samples collected on EDTA, obtained from  
328 the hematology department of the Toulouse hospital as left-over clinical material, for which we  
329 has consequently very little clinical information. For those samples, the HAT test was performed  
330 on whole blood, i.e. using the subjects' own RBCs for hemagglutination. The blood samples  
331 were subsequently centrifuged, and the plasmas collected to perform the Jurkat-S&R-flow  
332 and the RBD-ELISA tests.

333  
334 The result of the analysis of these two cohorts with the three serological tests are presented  
335 in Figure 2, with colors used to represent the HAT results.

336



337  
338

339 **Figure 2: Comparison of the results of the 3 serological tests on two cohorts of clinical samples.**  
340 Panel A: results obtained with a cohort of 121 serum samples (81 PCR pos, 40 neg) collected by the  
341 virology department of the Purpan Hospital (Toulouse, France).  
342 Panel B: results obtained with a cohort of 267 whole blood samples coming from the hematology  
343 department of the Rangueil Hospital (Toulouse, France).  
344 Each plot presents ELISA scores (Y axis) against the results of the Jurkat-S&R-flow tests, expressed as RSS.  
345 For improved clarity, both axes are presented on log scales (for this, the negative RSS values of 4 samples  
346 of the cohort on the right had to be manually converted to a value of 0.5).  
347 Colors are used to represent the HAT results: red: positive, blue: negative, yellow: partially positive  
348 hemagglutination, black: false positive, i.e. samples for which hemagglutination also occurred with the  
349 IH4 nanobody not coupled to the RBD domain.

350 The results of the first cohort (Figure 2A) show a clear-cut dichotomy in the distribution of  
351 the points, with two well separated clouds: one of blue points falling in the lower left quadrant,  
352 and one of red points in the upper right one. In other words, for this cohort of sera collected  
353 either from hospitalized Covid-19 patients or dating from before the pandemic for the negative  
354 controls, the three tests are in almost perfect agreement for the discrimination between  
355 positives and negatives, with just one yellow point in the lower right quadrant, i.e. positive for  
356 the Jurkat-S&R-flow test, showing only partial hemagglutination, but the signal for the RBD-  
357 ELISA test falling slightly below the threshold of 1 set by the manufacturer, suggesting that the  
358 anti-viral serological response of this subject was probably focused on regions of the spike  
359 protein outside of the RBD domain.

360  
361 Of note, partial hemagglutination was also recorded for two other samples which were  
362 negative for the two other tests. Those two samples were from a group of 38 patients  
363 hospitalized for Covid-19, but for whom the blood had been collected less than 14 days after the  
364 PCR diagnostic. This observation is in line with our previous observation that the HAT test may  
365 be particularly performant for the detection of early serological responses, probably because of  
366 a higher hemagglutinating capacity of IgMs (Townsend et al. 2021). Incidentally, in this same  
367 group of 'early' PCR-positive Covid patients, there were also 4 other samples which were  
368 negative for all three tests (see tables of data provided as supplementary material).

369  
370 The results of the second cohort, which comprised a few Covid patients, but also a large  
371 proportion of blood samples randomly picked among those from patients hospitalized for  
372 conditions unrelated to Covid-19, yielded a much less clear picture than the first one. As can be  
373 seen on Figure 2B, many of the dots for this cohort occupy a more intermediate position  
374 between the two clouds of clearly positive and clearly negative samples. In the upper right  
375 quadrant, one notices a relatively high proportion of blue and yellow spots, i.e. of HAT negative  
376 or partial samples in the set which were positive with both the RBD-ELISA and Jurkat-S&R-flow  
377 tests, albeit in the lower left part of the quadrant, i.e. rather weakly.

378  
379 On the other hand, there are also a handful of samples in the lower left quadrant for which  
380 partial or full hemagglutination was detected, which may correspond to early serological  
381 responses. There are also a few blue dots in the upper left and lower right quadrant, thus  
382 corresponding to samples being positive only either with the RBD ELISA or the Jurkat-S&R-flow  
383 test. According to previous work, the sera which react weakly on the full length spike protein  
384 expressed at the surface of Jurkat cells are most likely due to cross-reactivities with the S2  
385 domain of other coronaviruses (Ng et al. 2020; Khan et al. 2020).

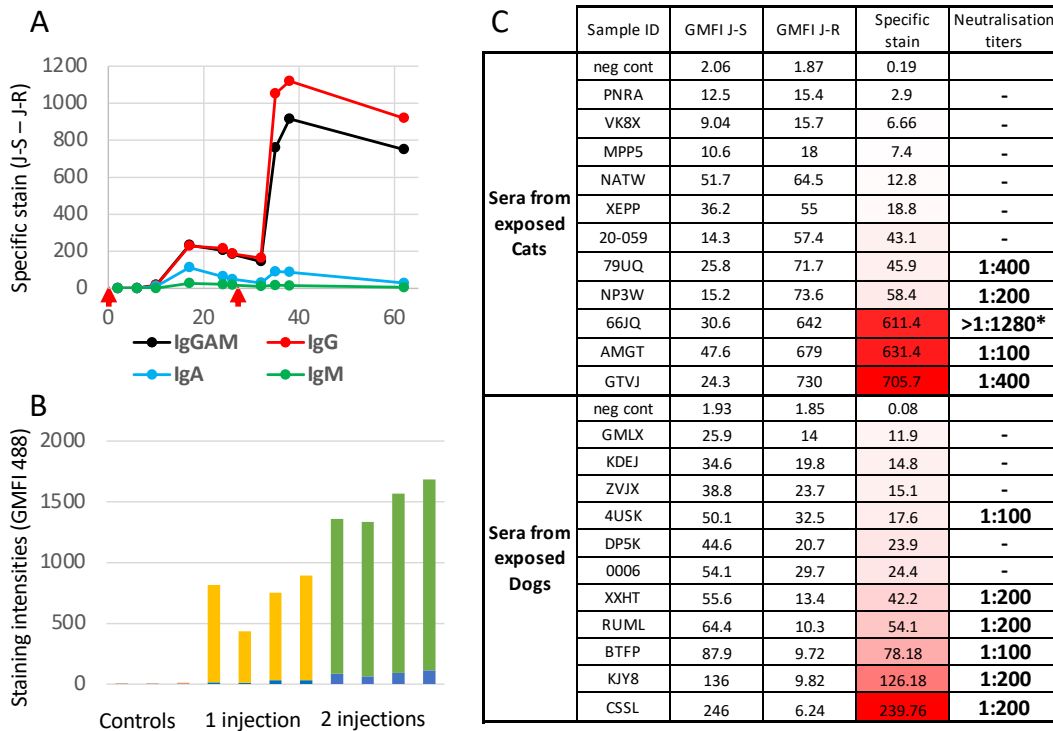
386  
387 One additional conclusion that can be drawn from the comparison of the results of the RBD-  
388 ELISA with those of the Jurkat-S&R-flow test is that, whilst the two methods show similar  
389 sensitivities, the ELISA signals tend to saturate very rapidly, and are thus much less dynamic than  
390 those obtained by flow cytometry.

391  
392

393 **Examples of possible uses of the Jurkat-S&R-flow test**

394  
 395 A further advantage of the Jurkat-S&R-flow test compared to the commercial RBD-ELISA we  
 396 used for this study is that it only requires 1 µL of plasma or serum, compared to 100 µL for the  
 397 ELISA, which makes it possible to perform on small volumes of capillary blood collected by finger  
 398 prick.  
 399

Figure 3



400 **Figure 3: Various examples of the possible uses of the Jurkat-S&R-flow test**

401 **Panel A: Monitoring serological responses in humans**

402  
 403 The Jurkat-S&R-flow test was used to follow the serological response of an individual during the  
 404 course of his vaccination (red arrows: first injection on day 0 and boost on day 27), with isotyping using  
 405 specific secondary reagents performed as described in the M&M section. Y axis: Specific staining ( GMFI  
 406 J-S – GMFI J-R)  
 407

408 **Panel B: The Jurkat-S&R-flow test can be used to follow Ig responses in mice.**

409  
 410 Sera from three groups of mice having been immunized either once, twice or not by intra-peritoneal  
 411 injection of inactivated SARS-CoV-2 virus were analyzed with the Jurkat-S&R-flow test, using an anti-  
 412 mouse Ig secondary antibody. Y axis: GMFI on Jurkat-R (blue columns), on Jurkat-S (top of green  
 413 columns), The specific signals correspond to the yellow or green portions (GMFI J-S – GMFI J-R).  
 414

415 **Panel C: In cats and dogs, the results of the Jurkat-S&R-flow test correlate with those of sero-  
 416 neutralization titers.**

417  
 418 Panels of sera from cats and dogs whose owners had recovered from symptomatic Covid-19 were  
 419 used to perform both sero-neutralization assays and the Jurkat-S&R-flow test, using the corresponding  
 420 secondary antibodies. Specific stain = GMFI J-S – GMFI J-R. \*: the higher SN titers shown for the cat  
 serum 66JQ was obtained on a different day from all the others.

421 As a proof of concept that this was doable and useful, we used capillary blood which one of  
422 the authors collected by pricking his finger at various intervals to document the time course of  
423 his serological response after vaccination, and the results are shown in panel A of Figure 3. One  
424 somewhat surprising finding was with the low levels of IgM recorded, which may in part be  
425 explained by the fact that, as a rule, anti-IgM secondary antibodies tend not to work as well as  
426 those against the other isotypes. One should note, however, that, with the same anti-IgM  
427 secondary reagent, signals of the same order of magnitude were found for IgG and IgM with the  
428 20/130 reference serum (Figure 1), as well as in several other samples (Table S1). The  
429 observation that the signals obtained with an anti-IgG reagent are similar, and even often a bit  
430 higher to those obtained with the pan-reactive anti-IgGAM is something which we tend to find  
431 in most samples (Table S1), and which had already been underlined by Grzelak et al. in the  
432 context of the S-flow test (Grzelak et al. 2020).

433  
434 The capacity of the SARS-CoV-2 virus to infect primates, hamsters or ferrets has provided  
435 very useful animal models to understand the physiopathology of Covid-19, whilst its capacity to  
436 infect domestic pets such as cats and dogs does raise concerns about the transmissions of the  
437 virus back to humans, as well as about the problem of animal reservoirs from which it will be  
438 very difficult to eradicate the virus. Whilst scores of commercial and lab-made methods have  
439 been described to follow human serological responses to the virus, there is a remarkable  
440 paucity of tests available today applicable to animals. Since all it would take to adapt the Jurkat-  
441 S&R-flow test to animals would be to use different species-specific secondary antibodies, we  
442 explored whether this would work for mice, cats, and dogs.

443  
444 First, we used sera of mice which had been immunized once or twice with inactivated SARS-  
445 CoV-2 virus injected intra-peritoneally. As can be seen on panel B of Figure 3, whilst the sera of  
446 control mice did not react significantly with Jurkat cells, those of immunized mice showed  
447 strong specific reactions against the spike protein, which were even higher in those having  
448 received two injections. Of note, the reactions against the Jurkat-R cells also went up in  
449 correlation with the injections, albeit to a much lesser degree than against the S protein. This is  
450 presumably due to the fact that the preparations of inactivated virus used for the  
451 immunizations probably contained some bovine proteins from the serum used in the tissue  
452 culture medium that would have the capacity to bind to the surface of the Jurkat cells, such as,  
453 for example, beta-2-microglobulin binding to MHC class I molecules. The Jurkat-S&R-flow  
454 method therefore seems to work very satisfactorily in mice, and since it requires only a few  $\mu\text{L}$   
455 of blood, it is well suited to follow serological responses over time.

456  
457 We then turned our attention to cats and dogs, which have both been shown to be  
458 susceptible to infections by the SARS-CoV-2 virus (Sit et al. 2020; Drózdź et al. 2021; Bessière et  
459 al. 2021; Chen 2020), but for which one of the only reliable means to test for the presence of a  
460 serological response is to perform sero-neutralization experiments, which are both  
461 cumbersome and require access to BSL-3 facilities. For our exploratory experiments, we simply  
462 used sets of sera collected from 11 cats and 11 dogs whose owners had had symptomatic Covid-  
463 19 infections, and on those we performed both sero-neutralization experiments, and the Jurkat-  
464 S&R-flow test, using the appropriate secondary antibodies. As can be seen on panel C of Figure  
465 3, we found a very good correlation between the levels of specific staining of Jurkat-S cells and  
466 the neutralization titers of the same sera. Whilst those are very preliminary observations which

467 will need to be strengthened by many more samples, and in particular with samples collected  
468 before the Covid-19 pandemic as negative controls, those results show that the Jurkat-S&R-flow  
469 test can clearly be used to evaluate the levels of antibodies against the S protein of the SARS-  
470 CoV-2 virus in cats and dogs, and could presumably also be adapted to other animals, be they  
471 pets, farm animals or laboratory models used to study the viral infection.

472

### 473 **Concluding remarks and perspectives**

474

475 Given its versatility, flexibility and affordability, we believe that the Jurkat-S&R-flow assay  
476 could prove useful for many research scientists wanting to measure serological responses  
477 directed towards the spike protein of the SARS-CoV-2 virus, either in humans, or in animals, but  
478 who would not have either the financial means to purchase commercial plate-based assays such  
479 as ELISA or CLIA, or access to the sizeable amounts of recombinant proteins required to set  
480 those up in-house. The Jurkat-S&R-flow test could be performed by any laboratory with access  
481 to tissue culture and to a flow cytometer, at a cost of roughly 10 cents per sample (see M&M for  
482 calculation). It is thus much cheaper than commercial ELISAs, which cost around 500 € per plate  
483 of 90 samples. And the Jurkat-S&R-flow test is also completely modular, i.e. each test only  
484 comprises the number of samples required, contrary to plate-based assays for which it is rather  
485 difficult not to use up a whole plate every time.

486

487 Several reports have already highlighted that using flow-cytometry for the detection of  
488 antibodies binding to the S protein expressed at the surface of cells tends to perform better  
489 than plate-based assays which use immobilized recombinant proteins (Egia-Mendikute et al.  
490 2021; Hambach et al. 2021; Lapuente et al. 2021; Goh et al. 2021; Horndler et al. 2021; Piñero et  
491 al. 2021; Grzelak et al. 2020; Ng et al. 2020). This is most likely related to the fact that many  
492 antibodies will be binding to conformational epitopes, which will only be found on the naturally  
493 expressed and properly folded spike protein. In this regard, the capacity of the S protein to  
494 undergo structural fluctuations, particularly at the level of the RBD domain which can be in  
495 either an open/up or closed/down conformation, has been shown to influence the binding-  
496 capacity of various antibodies (W. T. Harvey et al. 2021; Barnes et al. 2020; Robbiani et al. 2020;  
497 Piccoli et al. 2020; Zhou et al. 2020; Huang et al. 2021; Dejnirattisai et al. 2021). This is  
498 supported by the results shown in Figure S2, i.e. that, for most samples, we found that  
499 incubation at room temperature resulted in a sizeable increase in the amounts of antibodies  
500 binding to the spike-expressing cells, suggesting that, at the surface of live cells, the capacity of  
501 the spike protein to fluctuate between various conformations will expose different epitopes,  
502 and allow the binding of more antibodies.

503

504 One striking aspect of the results shown on Figure 2 is in the difference of performance of  
505 the tests between the two cohorts of samples tested. On the one hand, nearly perfect scores  
506 were obtained for all three tests on a cohort of sera comprised either of control samples  
507 collected before 2019, or of positive sera from PCR-positive Covid-19 patients. On the other  
508 hand, the situation was much less clear-cut for the cohort comprising blood samples picked  
509 more or less randomly and blindly among those available as left-overs from the hematology  
510 department and was, therefore, more akin to a 'real' population. For this second cohort, an  
511 additional confounding factor may have been that, since all the samples were from hospitalized

512 patients, some sera may have been poly-reactive due to inflammatory pathologies unrelated to  
513 Covid-19.

514  
515 All in all, this difference between the two cohorts is reminiscent of the common observation  
516 that the performances of clinical tests are often much lower on real populations than those  
517 obtained by the manufacturers on very carefully controlled and standardized populations. Our  
518 results indeed bring support to the view that the performance of any given serological test will  
519 be entirely dependent on the set of samples used to measure it: whilst it is relatively easy to  
520 reach an almost perfect score on a cohort comprised only of highly positive and completely  
521 negative samples such as the one used for Figure 2A, the situation becomes much less clear  
522 when using a set of samples more closely resembling the general population, in which the  
523 positive or negative nature of many samples will remain uncertain, and from which it would  
524 thus seem futile to try to make precise calculations of sensitivity and specificity. This being said,  
525 performing several tests in parallel on such cohorts is very useful to compare the performance  
526 of those tests with one another.

527  
528 Several recent reports have underlined the correlation between the serological levels of  
529 neutralizing antibodies, which are mostly directed against the RBD, and the degree of protection  
530 against becoming infected, or re-infected, by the SARS-Cov-2 virus (Feng et al. 2021; Khoury et  
531 al. 2021; Garcia-Beltran et al. 2021). Low levels of antibodies are often found in convalescent  
532 subjects following asymptomatic infections, and Kalamadasa and colleagues have shown that,  
533 whilst HAT sensitivity in such individuals can be as low as 50 %, HAT results are strongly  
534 correlated with the seroneutralisation activity in those samples (Kamaladasa et al. 2021). Over  
535 the coming months and years, antibodies levels will progressively decrease in both vaccinated  
536 and convalescent people, and one of the crucial questions will be that of when to start planning  
537 to administer vaccine boosts. Levels of neutralizing antibodies will certainly evolve very  
538 differently in different individuals, and an additional difficult aspect will be to define rules for  
539 the administration of vaccine boosts, and whether those should be defined as a general rule  
540 (e.g. so many months after the initial vaccination), or individually, based on the monitoring the  
541 levels of neutralizing antibodies. For such an individually-based approach, HAT would seem to  
542 be a particularly appropriate solution since it is a very simple and cheap test based on the  
543 binding of antibodies to the RBD domain (Townsend et al. 2021), which are those with  
544 neutralizing activity. Furthermore, because the only reagent in HAT simply comprises small  
545 amounts of soluble IH4-RBD protein, the hemagglutination test can be very easily adapted to  
546 detect antibodies binding to variant forms of the virus (Jayathilaka et al. 2021).

547 Whilst HAT is not as sensitive as an anti-RBD ELISA or the Jurkat-S&R-flow test, this relatively  
548 low sensitivity may not really be a problem for using HAT to help decide when to revaccinate  
549 people since low levels of antibodies are unlikely to be fully protective. By performing titrations,  
550 the HAT assay can also provide a quantitative assessment of the levels of circulating antibodies,  
551 which have been shown to correlate strongly with sero-neutralisation titers (Lamikanra et al.  
552 2021). In the current version of HAT, however, such a quantification can only be performed in a  
553 laboratory environment because it requires separation of the plasma or serum from the red  
554 blood cells. Making use of the Jurkat-S&R-flow test as a reference, we are currently in the  
555 process of completing work on a modified version of HAT that will be compatible with being  
556 performed pretty much anywhere, with no specialized equipment, and will provide a  
557 quantitative evaluation of the levels of antibodies in a single step (Joly et al. man in prep.).



558 **Detailed Contributions**

559

560 **Authors**

<b>Name</b>	<b>First name</b>	<b>ORCID</b>	<b>contributions</b>
Maurel Ribes	Agnes	<a href="https://orcid.org/0000-0002-7560-9502">0000-0002-7560-9502</a>	Collected and anonymized blood samples; scored HAT tests, corrected the manuscript
Bessière	Pierre	<a href="https://orcid.org/0000-0001-5657-0027">0000-0001-5657-0027</a>	Provided cat and dog sera; performed SN; helped perform FACS assays, corrected the manuscript
Guéry	Jean Charles	<a href="https://orcid.org/0000-0003-4499-3270">0000-0003-4499-3270</a>	Provided immunized mouse sera; corrected the manuscript
Joly Featherstone	Eloise	<a href="https://orcid.org/0000-0001-9077-359X">0000-0001-9077-359X</a>	Scored HAT tests
Bruel	Timothée	<a href="https://orcid.org/0000-0002-3952-4261">0000-0002-3952-4261</a>	Provided Jurkat-R and -S cells; corrected the manuscript
Robinot	Rémy	<a href="https://orcid.org/0000-0002-3651-0171">0000-0002-3651-0171</a>	Transduced, selected and grew Jurkat cells
Schwartz	Olivier	<a href="https://orcid.org/0000-0002-0729-1475">0000-0002-0729-1475</a>	Provided Jurkat-R and -S cells
Abravanel	Florence	<a href="https://orcid.org/0000-0002-1753-1065">0000-0002-1753-1065</a>	Provided cohort of sera and ELISA kits
Izopet	Jacques	<a href="https://orcid.org/0000-0002-8462-3234">0000-0002-8462-3234</a>	Provided cohort of sera and ELISA kits; made suggestions for the manuscript
Joly	Etienne	<a href="https://orcid.org/0000-0002-7264-2681">0000-0002-7264-2681</a>	Designed and funded the study; Performed the experiments; Wrote the paper.

561

562 **Other contributors**

Townsend	Alain	Designed the IH4-RBD reagent and funded its production
Tiong	Tan	Produced the IH4-RBD reagent
Rijal	Pramilla	Produced the IH4-RBD reagent
Buchrieser	Julian	Generated lentiviral vectors
Porrot	Françoise	Grew Jurkat cells
Featherstone	Carol	Copy edited parts of the manuscript

563

564 **Acknowledgements**

565

566 The authors are extremely grateful to Alain Townsend, Tiong Tan, Pramila Rajal, Julian  
567 Buchrieser and Françoise Porrot, who contributed the various materials detailed in the above  
568 table, and to Carol Featherstone for copy editing the manuscript. They also gratefully  
569 acknowledge the contributions of Marianne Navarra, for her help in setting up the agreement  
570 with the hospital; Miriam Pinilla, Karin Santoni and Etienne Meunier for the gift of Topro-3 and  
571 for performing the Mycoplasma tests; Emmanuelle Naser and Penelope Viana from the IPBS  
572 flow cytometry facility for their assistance, and the very helpful staff of the Toulouse EFS.

573

574 Funding: The first part of this project was funded by a private donation. The second part was  
575 funded by the ANR grant HAT-field to EJ.

576 **Materials and Methods**

577

578 **Reagents**

579

580 Polyclonal anti-human and anti-mouse Igs secondary antibodies, all conjugated to Alexa-488,  
581 were from Jackson laboratories, and purchased from Ozyme (France) . Refs: anti-human Ig-  
582 GAM: 109-545-064, -G: 109-545-003, -A: 109-54-011, -M: 109-545-129; anti-mouse Ig-G: 115-  
583 545-003

584

585 Anti-cat IgG (F4262) and anti-dog IgG (F7884) secondary antibodies, both conjugated to FITC,  
586 were obtained from Sigma.

587

588 Anti RBD monoclonal antibodies: F13A (site 1) and FD-11A (site 3) (Huang et al. 2021); C121  
589 (site 2) (Robbiani et al. 2020); CR3022 (site 4) (ter Meulen et al. 2006); EY6A (site 4) (Zhou et al.  
590 2020). All those were obtained using antibody-expression plasmids, as previously described  
591 (Townsend et al. 2021).

592

593 The 20/130 WHO reference serum was obtained from the NIBSC (Potters Bar, UK)

594

595 BSA Fraction V was obtained from Sigma (ref A8022).

596

597 PBS and tissue culture media were obtained from Gibco.

598

599 **Generation of Jurkat-S and Jurkat-R cell lines**

600 Both cell lines were obtained by means of lentiviral transduction.

601 pLV-EF1a-SARS-CoV-2-S-IRES-Puro was created by cloning a codon-optimized version of the  
602 SARS-CoV-2 S gene (GenBank: QHD43416.1) into the pLV-EF1a-IRES-Puro backbone (Addgene  
603 plasmid # 85132 ; <http://n2t.net/addgene:85132> ; RRID:Addgene\_85132) using BamHI and  
604 EcoRI sites.

605 The lentiviral vector for the expression of mCherry was obtained by replacing the GFP  
606 sequence of GFP by that of mCherry in the pCDH-EF1α-MCS\*-T2A-GFP plasmid  
607 ([https://systembio.com/shop/pcdh-ef1α-mcs-t2a-gfp-cdna-single-promoter-cloning-and-  
608 expression-lentivector/](https://systembio.com/shop/pcdh-ef1α-mcs-t2a-gfp-cdna-single-promoter-cloning-and-expression-lentivector/))

609 Lentiviral infectious supernatants were obtained after transient transfection of HEK cells with  
610 pLV- or pCDH-derived vectors, together with the packaging R8-2, and VSV-G plasmids.  
611 Supernatant was harvested 24h and 48h post transfection, passed through a 45 μm filter and  
612 stored in aliquots at -80°C. For the transduction of Jurkat cells, those were distributed in a 6 well  
613 plate at 1.5. 10<sup>6</sup> cell per well, in a volume of 500 μL of tissue culture medium (RPMI, 10 % FCS,  
614 1% PS, 2% Hepes), and 20 μL of the infectious supernatants were added, as well as 5 μL of  
615 Lentiblast premium (OZBiosciences). The plate was then spun at 1000g for 60 min at 32°C,  
616 before adding 2.5 ml of tissue culture medium and returning the plate to the 37°C incubator.  
617 Selection with puromycin was then performed at a concentration of 10μg/mL.

618 After a few days, the population of Jurkat cells thus obtained was stained for flow cytometry  
619 analysis using a highly reactive serum from a covid-19 patient, and it was found that most cells  
620 expressed the S protein, but at low to intermediate levels. To obtain a population that would  
621 express higher levels, we submitted this population to three successive rounds of sterile cell

622 sorting using a FACSAria Fusion cell sorter (Beckton Dickinson), selecting each time the 5 % of  
623 cells with the brightest staining. Cells were placed back in culture and reamplified after each  
624 round of selection. At the time of the second round of sorting, the cell sorter was also used for  
625 single cell cloning, but all of the dozen clones obtained by this means showed lower expression  
626 than the sorted population. The expression of the S protein in the population of Jurkat cells  
627 obtained after these three rounds of sorting was found to remain expressed in all cells, and at  
628 similar levels, for more than 50 successive passages, over many weeks of continuous cell  
629 culture.

630  
631 The Jurkat-R cells were obtained by successive transduction with the pCDH-GFP lentiviral  
632 vector described above, then with the empty pLV lentiviral vector, followed by selection with  
633 Puromycin at 10µg/mL. FACS analysis revealed that the mCherry fluorescent protein was  
634 expressed in 100 % of the cells of the population thus obtained, which therefore did not need to  
635 undergo any cell sorting.

636  
637 After the initial selection process, both the Jurkat-S and Jurkat-R cell line were maintained in  
638 RPMI, 10 % FCS, 2 mM Glutamine, 1% PS and Puromycin at 2.5 µg/mL. The Jurkat-S and Jurkat-R  
639 cell lines were both checked for the absence of mycoplasma contamination using the HEK blue  
640 hTLR2 kit (Invivogen, Toulouse, France)

#### 641 642 **FACS staining**

643 Before experiments, cells in the cultures of both Jurkat-S and Jurkat-R cell lines were  
644 counted, and sufficient numbers harvested to have a bit more than 10<sup>5</sup> cells of each per sample  
645 to be tested. Cells from both cell lines were then spun, and resuspended in their own tissue  
646 culture medium at a concentration of 2.2 10<sup>6</sup> cells/ mL before pooling equal volumes of the two.

647 Plasmas or sera to be tested were diluted 1/10, either in PBS or in PFN (PBS / 2% FCS / 200  
648 mg/L sodium azide ). 10 µL of these 1/10 dilutions were then placed in U-bottom 96 well plates,  
649 before adding 90 ul per well of the Jurkat-S&R mix.

650 The plates were then incubated for 30 minutes at room temperature before placing them on  
651 ice for a further 30 minutes. As can be seen on the supplementary Figure 2, we have found that  
652 this initial incubation at room temperature results in a marked increase of the staining signals  
653 for most antibodies.

654 All subsequent steps were carried out in the cold, with plates and washing buffers kept on  
655 ice. After the primary staining, samples were then washed in PFN, with resuspending the cells  
656 by tapping the plate after each centrifugation, and before adding the next wash. After 3 washes,  
657 one drop (i.e. ca. 30 ul) of secondary fluorescent antibody diluted 1/200 in PFN was added to  
658 each well, and the cells resuspended by gentle shaking of the plates.

659 After an incubation of 60 min on ice, samples were washed two more times with cold PFN  
660 before transferring the samples to acquisition tubes in a final volume of 300 ul PFN containing  
661 30 nM TO-PRO™-3 Iodide (Thermo Fischer Scientific, ref T3605).

662 This protocol was used for staining with just one pan-specific secondary antibody, i.e. for  
663 most of the samples of this study. For specific isotyping, i.e. for staining separately with either  
664 anti-IgG, -IgA or -IgM, as well as the pan-specific anti-Ig-GAM secondary antibody, we used  
665 double the quantities of cells and of serum or plasma for the primary step, and split the samples  
666 into 4 wells after the second wash, before proceeding to the subsequent steps as for the  
667 standard protocol.

668 The vast majority of the experiments for this study were analyzed on a FACScalibur flow  
669 cytometer controlled by the Cellquest pro software (Version 5.2, Beckton Dickinson), using the  
670 FL1 channel for Alexa-488 or FITC, the FL3 channel for m-Cherry, and the FL4 channel (with the  
671 633 nm laser) for live gating with the TO-PRO™-3 live stain.

672 For the samples shown on supplementary Figure 1, double quantities were used (as for  
673 isotyping) so that the same samples could also be acquired on a Fortessa flow cytometer,  
674 controlled by the Diva software (Beckton Dickinson). After the samples had been run on both  
675 machines, an equivalent volume of PBS with 2% formaldehyde what added to what was left in  
676 the tubes, and those were stored at 4°C for 4 days before they were once again analyzed on  
677 both machines.

678 Post-acquisition analysis of all the samples was performed using the Flowjo software (version  
679 10.7.1)

680

### 681 **Cost of the Jurkat-S&R-flow test**

682 The cost per sample of the Jurkat-S&R-flow test lies in large part with the price of the  
683 secondary antibodies used. Typically, one vial of secondary antibody costs about 150 € for 1ml,  
684 and using 30-50 ul at a 1/200 dilution will provide for at least 5000 samples. The cost of a  
685 polyclonal antibody is thus of the order or 3-5 cts per sample.

686 Each sample requires  $2 \cdot 10^5$  jurkat cells, which is roughly the amount obtained with 0.5 ml of  
687 standard tissue culture medium, which costs around 50 €/L, i.e. 2.5 cts/sample. All in all, if one  
688 adds the cost of TC, buffers for the washes and disposable plastics, we estimate that the cost  
689 per sample will be of the order of 10 cts.

690 The cost of access to a flow cytometer will be extremely variable between laboratories and  
691 institutes. If the cost of access is 20 € per hour, and one runs 200 samples per hour, this will add  
692 another 10 cts to the cost per sample.

693

### 694 **HAT tests**

695 HAT tests were performed using the IH4-RBD reagent diluted at 1 ug/ml in PBN rather than in  
696 straight PBS as originally described (Townsend et al. 2021), which results in a slight  
697 improvement of the HAT performances, and much improved stability of the IH4-RBD stocks (  
698 Joly et al., man in prep.). PBN simply consists of PBS complemented with 1% BSA and 200 mg/L  
699 sodium azide. The main role of BSA is to prevent the IH4-RBD reagent from adsorbing onto the  
700 plastic of tubes and assay plates, and the azide prevents bacterial and fungal contaminations of  
701 the stocks. HAT tests were all performed in V-bottom 96 wells plates (Sarstedt, ref 82 1583).

702 For performing HAT on sera, two tubes of suspension of RBC from an O- donor were  
703 prepared at approximately 6µL of packed RBC per ml of PBN. The first tube was used to fill the  
704 negative control wells with 90 µL per well. The IH4-RBD reagent was added at 1.1 ug/ml to the  
705 second tube of RBC suspension and this was dispensed at 90 µL per test well. Sera to be tested  
706 were diluted 1/10 in PBS, and 10 µL of the dilutions were added to a control and a test well.

707 For performing HAT on whole blood samples, which were all leftover clinical samples  
708 collected in EDTA tubes (purple tops), 10 µL were diluted with 60 µL of PBS + 5 mM EDTA, and  
709 10 µL of this 1/7 dilution were added to each of two wells containing either 90 µL of PBN for the  
710 negative controls, or 90 µL of PBN containing 1.1 µg/mL of IH4-RBD reagent for the test wells.  
711

712 For both sera and whole blood samples, after 60 minutes incubation at room temperature,  
713 the V bottom plates were placed on a homemade light box tilted at an angle of approximately  
714 10° from the vertical, and pictures taken with a mobile phone after approximately 20 seconds.

715 In an attempt to increase the sensitivity of the method by detecting partial  
716 hemagglutinations, the plates were then returned to a horizontal position for a further two  
717 hours, and the procedure of tilting the plate and taking pictures was repeated.

718 After transferring the pictures to computer files, the hemagglutination tests were scored by  
719 three independent assessors, of which two were blinded.

720 The scoring system was as follows: A score of 1 was given only to those samples which  
721 showed complete hemagglutination after one hour. A score of 0.5 was given to samples which  
722 showed either partial hemagglutination after one hour, or partial or complete hemagglutination  
723 after the second incubation of 2 hours.

724 This revealed that, whilst there was 100% agreement between the three assessors for the  
725 scoring of complete hemagglutination, the scoring of partial hemagglutination proved to be  
726 much more subjective and variable, and only those samples which had been scored as partials  
727 by all three assessors were finally considered as bona fide partial hemagglutinations.

728

## 729 **ELISA**

730 The ELISA tests were performed using the WANTAI SARS-CoV-2 Ab ELISA (ref WS-1096),  
731 according to the manufacturer's instructions. This commercial kit allows detection of all human  
732 antibody isotypes recognizing a recombinant RBD domain of the SARS-Cov-2 virus.

733 The ELISA tests for the cohort of 121 sera were performed in the virology department of the  
734 Toulouse hospital, as described previously (Abravanel et al. 2020).

735 The series of ELISA tests for the cohort of 267 plasmas were performed at the IPBS, with the  
736 washes being performed by hand rather than by an automated machine, and the 450/625 ODs  
737 read by a  $\mu$ Quant plate reader. All the positive samples of this cohort, as well as a set of  
738 randomly selected negatives, were submitted to a repeat of the assay, which showed excellent  
739 reproducibility.

740

## 741 **Human samples**

742 Purpan cohort: The collection of 2019 (negative) and SARS-CoV-2 infected (positive) patients  
743 was obtained from the laboratory of virology of the Purpan hospital, as previously described  
744 (Abravanel et al. 2020).

745 Ranguel Cohort: The samples were routine care residues from random patients, anonymized  
746 within 48 hours of collection, regardless of gender or hospitalization reason, collected in the  
747 course of a month between the end of January and the end of February 2021. The Covid status  
748 (PCR or positive serology) was unknown to the person performing the Jurkat-S&R-flow, ELISA  
749 and HAT experiments. Those whole blood samples were kept at room temperature until being  
750 used for HAT assays within 24 hours of obtaining them from the hospital. In trial experiments,  
751 we had found that such samples could be stored for up to 5 days without any noticeable  
752 difference in the performance of the HAT test.

753 After the whole blood samples had been used for HAT assays, the tubes were then spun, and  
754 the plasmas harvested into fresh tubes (to which sodium azide was added at a final  
755 concentration of 200  $\mu$ g/ml). Those harvested plasmas were kept at 4°C until they were used to  
756 perform the Jurkat-S&R-flow tests and ELISA tests.

757 Capillary blood: one of the authors of this study collected 50 µL of his own blood by finger  
758 pricking, using disposable lancets (Sarstedt ref 85.1016 ) on various days during the course of  
759 his vaccination regimen with the Pfizer/BioNTech vaccine. At the time of collection, the blood  
760 samples were diluted with 200 µL of PBS + 5mM EDTA (Since whole blood is roughly 50% RBCs  
761 and 50% plasma, this 1/5 dilution of the blood actually corresponds to a 1/10 dilution of the  
762 plasma). The plasma was then separated from the RBCs after centrifugation, placed in another  
763 tube with sodium azide, and stored at 4°C until the day of the assay.

764

## 765 **Experiments on mouse sera**

### 766 Virus preparation and inactivation

767 SARS-CoV2 was grown on Vero E6 cells (ATCC) in DMEM (Dutscher) supplemented with  
768 100 U/mL penicillin, 100 µg/ml streptomycin (Invitrogen), and 2% heat inactivated fetal bovine  
769 serum (Sigma). Viral stocks were propagated in 300 cm<sup>2</sup> flasks (Dutscher) in which 10<sup>3</sup> tissue  
770 culture infectious dose 50 (TCID<sub>50</sub>) were inoculated in 100 ml of medium for 3 days at 37°C with  
771 5% CO<sub>2</sub>. Culture supernatants containing the viral stocks were harvested and inactivated with  
772 BPL (Fischer) overnight at 4°C. Virus was then concentrated by ultracentrifugation at 25 000 rpm  
773 (for 2 hours at 4°C) on a 20% sucrose cushion in Ultra-Clear centrifuge tubes (SW-32 Ti rotor,  
774 Beckman). Pellets were resuspended in PBS, protein concentration was quantified by BCA  
775 Protein Assay kit (Pierce). BPL-inactivated SARS-CoV2 stocks at protein concentrations ranging  
776 from 1 to 5 µg/µL were stored at -80°C until use.

### 777 Mouse immunization

778 Mice were injected intra-peritoneally with 15 µg of BPL-SARS-CoV2 in 250 µl of PBS, and then  
779 challenged with the same amount at day 62. Mice were euthanized and serum was collected at  
780 day 14 post-primary immunization and at day 7 post-secondary challenge.

781

## 782 **Experiments on Cat and Dog sera**

783 Serum samples were collected from cats and dogs belonging to owners who developed COVID-  
784 19-like symptoms and subsequently tested positive for SARS-CoV-2 infection by RT-qPCR. , at least  
785 one month after the owners' recoveries. Samples and data collections were conducted according  
786 to the guidelines of the Declaration of Helsinki, and approved by the Ethics Committee Sciences  
787 et Santé Animale n°115 (protocol code COVIFEL approved on 1 September 2020, registered under  
788 SSA\_2020\_010).

### 789 Sero-neutralisation assay

790 Serum samples and controls were heat-inactivated at 56 °C for 30 min, serially diluted in  
791 DMEM starting at 1:10, mixed with an equal volume of SARS-CoV-2 stock (previously amplified  
792 and titrated on Vero-E6 cells and diluted in DMEM to contain 2000 TCID<sub>50</sub>/ml), incubated for 2  
793 hours at 37 °C, and 100 µL transferred to tissue-culture 96 well plates plated with 12.000 Vero-  
794 E6 cells per well the day before the assay, in DMEM complemented with 10% of heat-  
795 inactivated fetal bovine serum and 1% of penicillin-streptomycin at 37 °C with 5% of CO<sub>2</sub>  
796 (medium was removed before adding the virus-serum dilutions). After 60 minutes at 37°C, the  
797 virus-serum dilutions were removed before adding DMEM complemented with 2% of heat-  
798 inactivated fetal bovine serum and 1% of penicillin-streptomycin. Cells were then incubated for  
799 72 h at 37 °C with 5% of CO<sub>2</sub>. Individual wells were then screened by eye under the microscope  
800 for cytopathic effects. Monoclonal anti-SARS-CoV CR3022 antibody (BEI Resources, NIAID, NIH)  
801 was used as a positive control. PBS was used as a negative control. Experiments were carried  
802 out in a biosafety level 3 facility at the National Veterinary School of Toulouse.



803 **Ethical statement**

804 All sera from the first cohort, and whole blood samples from the second cohort, were  
805 obtained from the Toulouse hospital, where all patients give, by default, their consent for any  
806 biological material left over to be used for research purposes after all the clinical tests  
807 requested by doctors have been duly completed. Material transfer was done under a signed  
808 agreement (CNRS n° 227232, CHU n° 20 427 C). This study was declared and approved by the  
809 governing body of the Toulouse University Hospital with the agreement number RnIPH 2021-99,  
810 confirming that ethical requirements were fully respected.

811  
812 Using such materials, we did not really have control over how representative our cohorts  
813 may be, but this allowed us to circumvent the very stringent rules set by French laws regarding  
814 the use of human materials for research (RIPH, Loi Jardé). Under those rules, setting up a clinical  
815 trial involving biological materials of human origin would require many months of  
816 administrative procedures and paperwork, as well as several hundreds of thousands of euros,  
817 which we did not have access to.

818

819 **Bibliography**

- 820 Abravanel, F., Miédouge, M., Chapuy-Regaud, S., Mansuy, J.-M. and Izopet, J. 2020. Clinical  
821 performance of a rapid test compared to a microplate test to detect total anti SARS-CoV-2  
822 antibodies directed to the spike protein. *Journal of Clinical Virology* 130, p. 104528.
- 823 Abu-Raddad, L.J., Chemaitelly, H., Coyle, P., et al. 2021. SARS-CoV-2 reinfection in a cohort of  
824 43,000 antibody-positive individuals followed for up to 35 weeks. *medRxiv*.
- 825 Adams, E.R., Ainsworth, M., Anand, R., et al. 2020. Antibody testing for COVID-19: A report  
826 from the National COVID Scientific Advisory Panel. *Wellcome Open Research* 5, p. 139.
- 827 Amanat, F., Stadlbauer, D., Strohmeier, S., et al. 2020. A serological assay to detect SARS-CoV-  
828 2 seroconversion in humans. *Nature Medicine* 26(7), pp. 1033–1036.
- 829 Barnes, C.O., Jette, C.A., Abernathy, M.E., et al. 2020. SARS-CoV-2 neutralizing antibody  
830 structures inform therapeutic strategies. *Nature* 588(7839), pp. 682–687.
- 831 Bessière, P., Fusade-Boyer, M., Walch, M., et al. 2021. Household Cases Suggest That Cats  
832 Belonging to Owners with COVID-19 Have a Limited Role in Virus Transmission. *Viruses*  
833 13(4).
- 834 Chen, H. 2020. Susceptibility of ferrets, cats, dogs, and different domestic animals to SARS-  
835 coronavirus-2. *BioRxiv*.
- 836 Chen, Xinhua, Chen, Z., Azman, A.S., et al. 2021. Serological evidence of human infection with  
837 SARS-CoV-2: a systematic review and meta-analysis. *The Lancet. Global health* 9(5), pp.  
838 e598–e609.
- 839 Dejnirattisai, W., Zhou, D., Ginn, H.M., et al. 2021. The antigenic anatomy of SARS-CoV-2  
840 receptor binding domain. *Cell* 184(8), p. 2183–2200.e22.
- 841 Dortet, L., Ronat, J.-B., Vauloup-Fellous, C., et al. 2021. Evaluating 10 Commercially Available  
842 SARS-CoV-2 Rapid Serological Tests by Use of the STARD (Standards for Reporting of  
843 Diagnostic Accuracy Studies) Method. *Journal of Clinical Microbiology* 59(2).
- 844 Drózdź, M., Krzyżek, P., Dudek, B., Makuch, S., Janczura, A. and Paluch, E. 2021. Current State  
845 of Knowledge about Role of Pets in Zoonotic Transmission of SARS-CoV-2. *Viruses* 13(6).
- 846 Egia-Mendikute, L., Bosch, A., Prieto-Fernández, E., et al. 2021. Sensitive detection of SARS-  
847 CoV-2 seroconversion by flow cytometry reveals the presence of nucleoprotein-reactive  
848 antibodies in unexposed individuals. *Communications Biology* 4(1), p. 486.
- 849 Fani, M., Teimoori, A. and Ghafari, S. 2020. Comparison of the COVID-2019 (SARS-CoV-2)  
850 pathogenesis with SARS-CoV and MERS-CoV infections. *Future virology*.

851 Farnsworth, C.W. and Anderson, N.W. 2020. SARS-CoV-2 Serology: Much Hype, Little Data.  
852 *Clinical Chemistry* 66(7), pp. 875–877.

853 Feng, S., Phillips, D.J., White, T., et al. 2021. Correlates of protection against symptomatic and  
854 asymptomatic SARS-CoV-2 infection. *medRxiv*.

855 Garcia-Beltran, W.F., Lam, E.C., Astudillo, M.G., et al. 2021. COVID-19-neutralizing antibodies  
856 predict disease severity and survival. *Cell* 184(2), p. 476–488.e11.

857 Goh, Y.S., Ng, L.F.P. and Renia, L. 2021. A flow cytometry-based assay for serological  
858 detection of anti-spike antibodies in COVID-19 patients. *STAR Protocols* 2(3), p. 100671.

859 Grzelak, L., Temmam, S., Planchais, C., et al. 2020. A comparison of four serological assays for  
860 detecting anti-SARS-CoV-2 antibodies in human serum samples from different populations.  
861 *Science Translational Medicine* 12(559).

862 Hambach, J., Stähler, T., Eden, T., et al. 2021. A simple, sensitive, and low-cost FACS assay for  
863 detecting antibodies against the native SARS-CoV-2 spike protein. *Immunity, inflammation  
864 and disease* 9(3), pp. 905–917.

865 Harvey, R.A., Rassen, J.A., Kabelac, C.A., et al. 2021. Association of SARS-CoV-2 Seropositive  
866 Antibody Test With Risk of Future Infection. *JAMA internal medicine* 181(5), pp. 672–679.

867 Harvey, W.T., Carabelli, A.M., Jackson, B., et al. 2021. SARS-CoV-2 variants, spike mutations  
868 and immune escape. *Nature Reviews. Microbiology* 19(7), pp. 409–424.

869 Hickey, M.J., Valenzuela, N.M. and Reed, E.F. 2016. Alloantibody generation and effector  
870 function following sensitization to human leukocyte antigen. *Frontiers in immunology* 7, p.  
871 30.

872 Horndler, L., Delgado, P., Abia, D., et al. 2021. Flow cytometry multiplexed method for the  
873 detection of neutralizing human antibodies to the native SARS-CoV-2 spike protein. *EMBO  
874 Molecular Medicine* 13(3), p. e13549.

875 Huang, K.-Y.A., Tan, T.K., Chen, T.-H., et al. 2021. Breadth and function of antibody response  
876 to acute SARS-CoV-2 infection in humans. *PLoS Pathogens* 17(2), p. e1009352.

877 Jayathilaka, D., Jeewandara, C., Gomes, L., et al. 2021. Comparison of kinetics of immune  
878 responses to SARS-CoV-2 proteins in individuals with varying severity of infection and  
879 following a single dose of the AZD1222. *medRxiv*.

880 Jeewandara, C., Kamaladasa, A., Pushpakumara, P.D., et al. 2021. Immune responses to a single  
881 dose of the AZD1222/Covishield vaccine in health care workers. *Nature Communications*  
882 12(1), p. 4617.

883 Jeffery-Smith, A., Iyanger, N., Williams, S.V., et al. 2021. Antibodies to SARS-CoV-2 protect  
884 against re-infection during outbreaks in care homes, September and October 2020. *Euro  
885 Surveillance* 26(5).

886 Kamaladasa, A., Gunasekara, B., Jeewandara, C., et al. 2021. Comparison of two assays to detect  
887 IgG antibodies to the receptor binding domain of SARS-CoV-2 as a surrogate marker for  
888 assessing neutralizing antibodies in COVID-19 patients. *International Journal of Infectious  
889 Diseases* 109, pp. 85–89.

890 Karahan, G.E., Claas, F.H.J. and Heidt, S. 2020. Pre-existing Alloreactive T and B Cells and  
891 Their Possible Relevance for Pre-transplant Risk Estimation in Kidney Transplant Recipients.  
892 *Frontiers in medicine* 7, p. 340.

893 Khan, S., Nakajima, R., Jain, A., et al. 2020. Analysis of Serologic Cross-Reactivity Between  
894 Common Human Coronaviruses and SARS-CoV-2 Using Coronavirus Antigen Microarray.  
895 *BioRxiv*.

896 Khoury, D.S., Cromer, D., Reynaldi, A., et al. 2021. Neutralizing antibody levels are highly  
897 predictive of immune protection from symptomatic SARS-CoV-2 infection. *Nature Medicine*  
898 27(7), pp. 1205–1211.

899 Koopmans, M. and Haagmans, B. 2020. Assessing the extent of SARS-CoV-2 circulation

900 through serological studies. *Nature Medicine* 26(8), pp. 1171–1172.

901 Lamikanra, A., Nguyen, D., Simmonds, P., et al. 2021. Comparability of six different  
902 immunoassays measuring SARS-CoV-2 antibodies with neutralising antibody levels in  
903 convalescent plasma: from utility to prediction. *Transfusion*.

904 Lapuente, D., Maier, C., Irrgang, P., et al. 2021. Rapid response flow cytometric assay for the  
905 detection of antibody responses to SARS-CoV-2. *European Journal of Clinical Microbiology  
906 & Infectious Diseases* 40(4), pp. 751–759.

907 Letizia, A.G., Ge, Y., Vangeti, S., et al. 2021. SARS-CoV-2 Seropositivity and Subsequent  
908 Infection Risk in Healthy Young Adults: A Prospective Cohort Study. *SSRN Electronic  
909 Journal*.

910 Long, Q.-X., Tang, X.-J., Shi, Q.-L., et al. 2020. Clinical and immunological assessment of  
911 asymptomatic SARS-CoV-2 infections. *Nature Medicine* 26(8), pp. 1200–1204.

912 Lumley, S.F., O'Donnell, D., Stoesser, N.E., et al. 2021. Antibody Status and Incidence of  
913 SARS-CoV-2 Infection in Health Care Workers. *The New England Journal of Medicine*  
914 384(6), pp. 533–540.

915 ter Meulen, J., van den Brink, E.N., Poon, L.L.M., et al. 2006. Human monoclonal antibody  
916 combination against SARS coronavirus: synergy and coverage of escape mutants. *PLoS  
917 Medicine* 3(7), p. e237.

918 Mohit, E., Rostami, Z. and Vahidi, H. 2021. A comparative review of immunoassays for COVID-  
919 19 detection. *Expert review of clinical immunology*.

920 Moshe, M., Daunt, A., Flower, B., et al. 2021. SARS-CoV-2 lateral flow assays for possible use  
921 in national covid-19 seroprevalence surveys (React 2): diagnostic accuracy study. *BMJ  
922 (Clinical Research Ed.)* 372, p. n423.

923 Ng, K.W., Faulkner, N., Cornish, G.H., et al. 2020. Preexisting and de novo humoral immunity to  
924 SARS-CoV-2 in humans. *Science* 370(6522), pp. 1339–1343.

925 Piccoli, L., Park, Y.-J., Tortorici, M.A., et al. 2020. Mapping Neutralizing and Immunodominant  
926 Sites on the SARS-CoV-2 Spike Receptor-Binding Domain by Structure-Guided High-  
927 Resolution Serology. *Cell* 183(4), p. 1024–1042.e21.

928 Piñero, P., Marco De La Calle, F.M., Horndler, L., et al. 2021. Flow cytometry detection of  
929 sustained humoral immune response (IgG + IgA) against native spike glycoprotein in  
930 asymptomatic/mild SARS-CoV-2 infection. *Scientific Reports* 11(1), p. 10716.

931 Robbiani, D.F., Gaebler, C., Muecksch, F., et al. 2020. Convergent antibody responses to SARS-  
932 CoV-2 in convalescent individuals. *Nature* 584(7821), pp. 437–442.

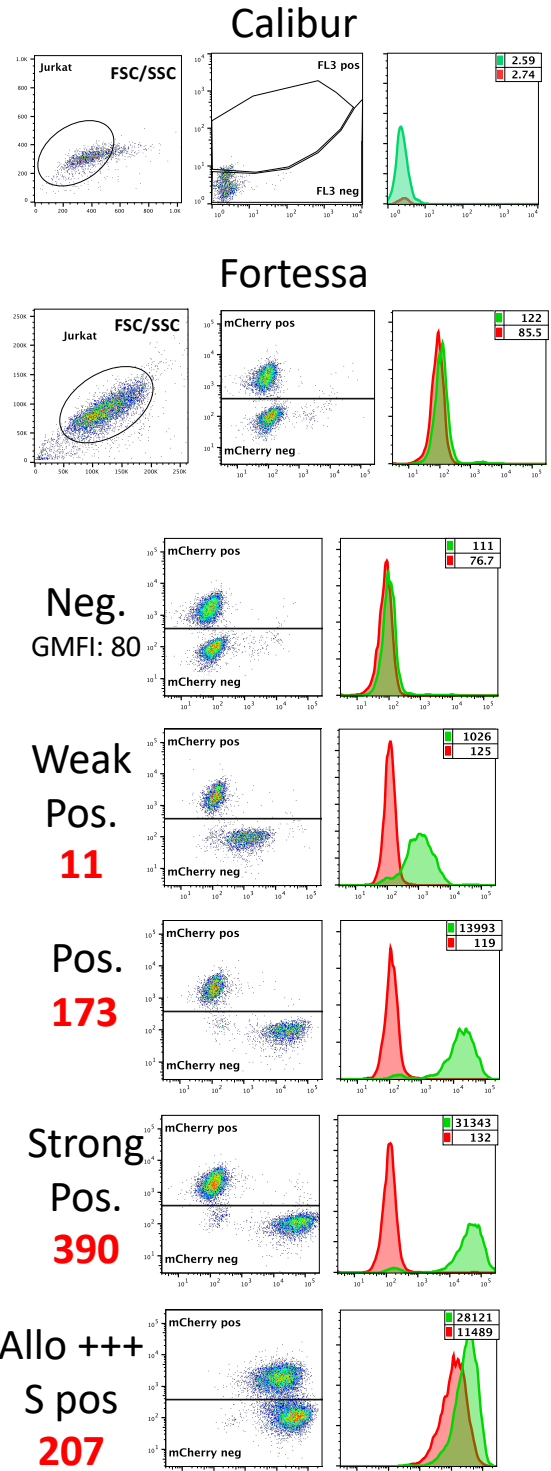
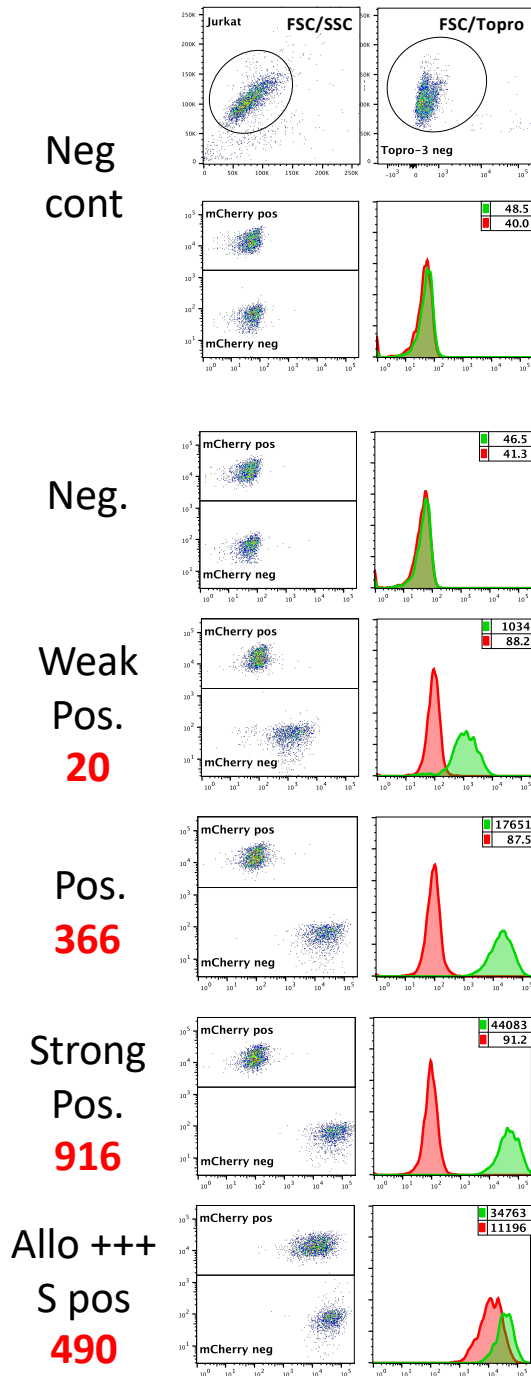
933 Sit, T.H.C., Brackman, C.J., Ip, S.M., et al. 2020. Infection of dogs with SARS-CoV-2. *Nature*  
934 586(7831), pp. 776–778.

935 Townsend, A., Rijal, P., Xiao, J., et al. 2021. A haemagglutination test for rapid detection of  
936 antibodies to SARS-CoV-2. *Nature Communications* 12(1), p. 1951.

937 Wu, Z., Harrich, D., Li, Z., Hu, D. and Li, D. 2021. The unique features of SARS-CoV-2  
938 transmission: Comparison with SARS-CoV, MERS-CoV and 2009 H1N1 pandemic influenza  
939 virus. *Reviews in medical virology* 31(2), p. e2171.

940 Zhou, D., Duyvesteyn, H.M.E., Chen, C.-P., et al. 2020. Structural basis for the neutralization of  
941 SARS-CoV-2 by an antibody from a convalescent patient. *Nature Structural & Molecular  
942 Biology* 27(10), pp. 950–958.

Figure S1



Fixed 1% formaldehyde, 4 days @ 4°C

947 **Figure S1: Using a flow cytometer with a 561 nm Yellow-Green laser improves the mCherry**  
948 **signals**

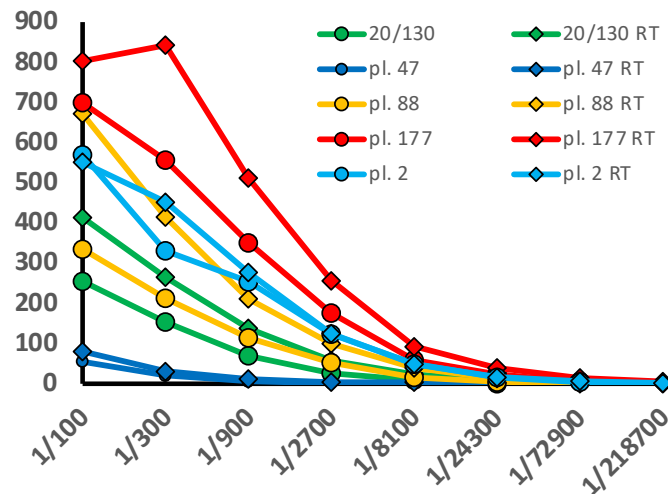
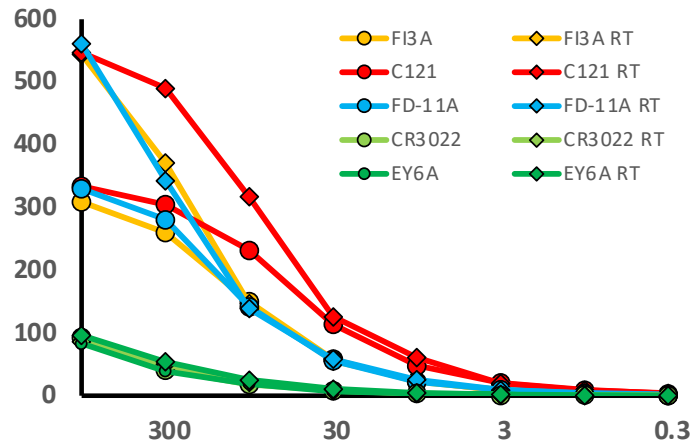
949 The same samples shown on Figure 1 were also analyzed on a Fortessa flow cytometer. The  
950 561 nm yellow-green laser was used for the excitation of the mCherry fluorescent protein,  
951 which led to much brighter signals, and thus to much easier separation of the Jurkat-R (mCherry  
952 pos) and Jurkat-S (mCherry neg) populations than when the samples were acquired on a  
953 FACScalibur.

954 As in figure 1, the numbers in the upper right corners of the histogram overlays plots  
955 correspond to the GMFI of the two histograms (Red: Jurkat-R; green: Jurkat-S), and the big red  
956 numbers to the left of the plots to the RSS. Of note, although the GMFI values were much higher  
957 on the Fortessa than those recorded on the FACScalibur, the RSS values of the various samples  
958 were all very similar between the two machines.

959  
960 After the samples had been run on both flow cytometers, those were fixed in 1%  
961 formaldehyde by adding an equal volume of PBS + 2% formaldehyde to the remainder of each  
962 sample. The tubes were then stored à 4°C for 4 days before re-analyzing them on both  
963 cytometers. As can be seen on the right hand side of the figure, the red fluorescence of the  
964 mCherry was still detectable on the Fortessa after this procedure of fixation, despite the  
965 intensity of the signals having dropped by about 7 fold. On the FACScalibur, however, this drop  
966 of the mCherry fluorescent signals precluded the separation of the Jurkat-S from the Jurkat-R  
967 cells. If samples are to be fixed, performing the Jurkat-R&S-flow test will thus require access to a  
968 flow cytometer equipped with a 561 nm Yellow-Green laser. As an alternative, we are currently  
969 exploring the possibility of transforming the Jurkat-S&R-flow test into a Jurkat-S&G-flow test,  
970 where the negative control cells would be expressing GFP, which is excited at 488 nm, and using  
971 secondary antibodies conjugated to red fluorochromes such as Alexa647, excited by a 633 nm  
972 red laser, for the detection of the primary antibodies.

973  
974 Of note, in the dot plots of the Positive and Strong Positive fixed samples, faint clouds of FL1  
975 negative cells can be seen in the mCherry neg window. Those presumably correspond to Jurkat-  
976 R cells which were dead before the fixation step, and from which the mCherry had thus leaked  
977 out. When analyzing populations of live cells, such cells are gated out with the To-pro 3 live  
978 stain, but this no longer works for population of fixed cells. This small problem could probably  
979 be circumvented using a fixable dead cell staining dye such as the LIVE/DEAD Fixable Far Red  
980 stain (ThermoFischer L34973).

981  
982



983  
984

985 **Figure S2:** Incubation of the samples at room temperature for the first part of the primary  
986 staining step markedly improves the staining signals for most antibodies.

987 For a large fraction of monoclonal and polyclonal antibodies reacting with the Spike protein  
988 expressed at the surface of cells, we have repeatedly observed that a step of incubation at room  
989 temperature can result in a marked improvement of the staining signals compared to  
990 performing the staining continuously on ice.

991 For this experiment, we selected a panel of 5 monoclonal antibodies reacting with different  
992 sites of the spike RBD domain, a panel of 4 plasmas reacting with various intensities, as well the  
993 20/130 reference serum.

994 For all the samples, we performed eight steps of 3-fold dilutions, and placed 10 ul of the  
995 diluted samples in two parallel U bottom 96 well plates. The first plate was kept at room  
996 temperature (RT) whilst the other one was placed on ice. The Jurkat-S&R mix was then added to  
997 the wells of the plate at room temperature. The tube was then placed on ice for a few minutes,  
998 before distributing the mix in the wells of the second plate. After 30 minutes, the plate which  
999 had been sitting at room temperature was also placed on ice, and incubated for another 30  
1000 minutes. The rest of the staining procedure was then exactly the same for the two plates, all  
1001 performed in the cold as described in M&M.  
1002



	Sample ID	IgGAM			IgG			IgA			IgM			G+A+M	Fraction IgG signal	Fraction IgA signal	Fraction IgM signal
		GMFI Jurkat R	GMFI Jurkat S	specific stain S - J-R (J <sub>r</sub> )	GMFI Jurkat R	GMFI Jurkat S	specific stain S - J-R (J <sub>r</sub> )	GMFI Jurkat R	GMFI Jurkat S	specific stain S - J-R (J <sub>r</sub> )	GMFI Jurkat R	GMFI Jurkat S	specific stain S - J-R (J <sub>r</sub> )				
Sera	neg	1.87	2.01	0.14	1.95	1.99	0.04	1.79	2.13	0.34	1.89	1.98	0.09	0.47			
	30/120	3.19	760	756.81	3.59	763	759.41	2.11	63.2	61.09	2.74	640	637.26	1457.76	0.52	0.04	0.44
	<J14-3	5.1	51.6	46.5	7.47	57.2	49.73	3.08	29.1	26.02	2.55	8.65	6.1	81.85	0.61	0.32	0.07
	<J14-29	4.59	738	733.41	5.16	919	913.84	2.77	122	119.23	2.54	203	200.46	1233.53	0.74	0.10	0.16
	<J14-32	4.71	1692	1687.29	5.25	2350	2344.75	4.01	610	605.99	2.56	402	399.44	3350.18	0.70	0.18	0.12
	<J14-35	4.65	198	193.35	4.82	209	204.18	1.97	52.6	50.63	3.14	13.1	9.96	264.77	0.77	0.19	0.04
	<J14-109	6.52	852	845.48	6.23	1082	1075.77	2.61	179	176.39	4.55	126	121.45	1373.61	0.78	0.13	0.09
	<J14-130	8.7	150	141.3	9.46	151	141.54	3.28	45.7	42.42	5.25	58.1	52.85	236.81	0.60	0.18	0.22
	>J14-40	4.84	54.9	50.06	6.07	54.3	48.23	2.18	12	9.82	2.76	29.1	26.34	84.39	0.57	0.12	0.31
	neg-2213	10.5	33.3	22.8	12.3	43.3	31	3.21	6.58	3.37	6.12	8.77	2.65	37.02	0.84	0.09	0.07
	neg-2649	19.2	41.4	22.2	24.7	56.2	31.5	6.32	9.59	3.27	6.15	9.62	3.47	38.24	0.82	0.09	0.09
	Plasmas	2	438	1427	989	577	1846	1269	59.4	469	409.6	739	1333	594	2272.60	0.56	0.18
18		7.82	84.9	77.08	11.3	101	89.7	2.67	33.4	30.73	4.89	12.7	7.81	128.24	0.70	0.24	0.06
19		2.02	2.2	0.18	2.07	2.15	0.08	1.82	2.18	0.36	1.83	1.96	0.13	0.57			
36		4.53	88.7	84.17	5.01	90.2	85.19	2.38	48.5	46.12	3.61	10.4	6.79	138.10	0.62	0.33	0.05
47		3.47	139	135.53	3.65	141	137.35	2.15	47.1	44.95	2.8	42.2	39.4	221.70	0.62	0.20	0.18
56		9.03	25.7	16.67	9.48	26.8	17.32	2.56	17.2	14.64	7.16	11.2	4.04	36.00	0.48	0.41	0.11
57		5.84	25.5	19.66	7.04	26.7	19.66	2.17	8.87	6.7	4.55	13.9	9.35	35.71	0.55	0.19	0.26
73		3.87	130	126.13	3.61	159	155.39	1.91	4.35	2.44	3.1	4.64	1.54	159.37	0.98	0.02	0.01
80		2.5	82	79.5	3.07	99.1	96.03	2.06	2.75	0.69	2.21	2.56	0.35	97.07	0.99	0.01	0.00
83		3.13	1674	1670.87	3.69	1900	1896.31	2.21	542	539.79	2.4	629	626.6	3062.70	0.62	0.18	0.20
88		3.74	1110	1106.26	4.18	1297	1292.82	2.51	159	156.49	3.03	632	628.97	2078.28	0.62	0.08	0.30
108		3.53	7.65	4.12	4.22	9.66	5.44	2.08	2.61	0.53	2.6	3.58	0.98	6.95			
123		54.5	75.6	21.1	51.6	71.4	19.8	4.22	6.14	1.92	43.5	61.1	17.6	39.32	0.62	0.08	0.30
161		2.91	5.84	2.93	6.17	11.1	4.93	2.08	2.59	0.51	2.09	2.25	0.16	5.60			
166		101	162	61	109	176	67	27.2	35.3	8.1	46.5	68.9	22.4	97.50	0.69	0.08	0.23
174		3.11	190	186.89	4.43	228	223.57	2.45	50.1	47.65	2.19	42.3	40.11	311.33	0.72	0.15	0.13
177		7.9	1945	1937.1	8.04	2303	2294.96	2.32	581	578.68	7.58	699	691.42	3565.06	0.64	0.16	0.19
227		4.12	77	72.88	5.31	51.4	46.09	2.83	6.19	3.36	3	73.8	70.8	120.25	0.38	0.03	0.59
232		11	131	120	12.6	169	156.4	6.21	9.13	2.92	4.84	6.83	1.99	161.31	0.97	0.02	0.01
241		4.11	2411	2406.89	4.61	2860	2855.39	2.6	608	605.4	2.83	47.8	44.97	3505.76	0.81	0.17	0.01
247	13.8	23.3	9.5	21.6	31.7	10.1	8.87	15.7	6.83	3.5	5.88	2.38	19.31	0.52	0.35	0.12	
253	3.98	28.2	24.22	5.22	33	27.78	2.43	10.7	8.27	2.43	2.9	0.47	36.52	0.76	0.23	0.01	
260	23.2	33.9	10.7	30.8	44.1	13.3	29.4	43	13.6	5.98	7.61	1.63	28.53	0.47	0.48	0.06	

1003

1004 **Table S1:** Example of isotyping performed on a representative set of various serum and  
 1005 plasma samples.

1006 As can be seen on the right hand side portion of the table, comparison of samples from  
 1007 different patients shows that there can be large variations in the proportions of Ig-G,-A and -M.  
 1008 Because polyclonal secondary antibodies will not all react with their targeted primary antibodies  
 1009 with the same efficiency, however, the actual signals for the various subclasses of antibodies  
 1010 should not be taken as a true reflection of the amounts of each subclass of antibody.

1011 If a more quantitative evaluation was needed, monoclonal secondary antibodies could be  
 1012 used instead of polyclonal reagents, making sure that all those isotypes-specific secondary  
 1013 monoclonal antibodies were being used well above the saturating concentration, and  
 1014 conjugated to similar amounts of the same fluorochrome. This would, however, increase the  
 1015 cost of the procedure considerably.

1016